IEEE Photonics Journal
An IEEE Photonics Society Publication

Open Access

Equalization-Enhanced Phase Noise in Stokes-Vector Direct Detection Systems

Volume 8, Number 6, December 2016

Meng Qiu
Qunbi Zhuge
Mohammed Y. S. Sowailem
Thang M. Hoang
Mathieu Chagnon
Meng Xiang
Xingyu Zhou
Fangyuan Zhang
David V. Plant

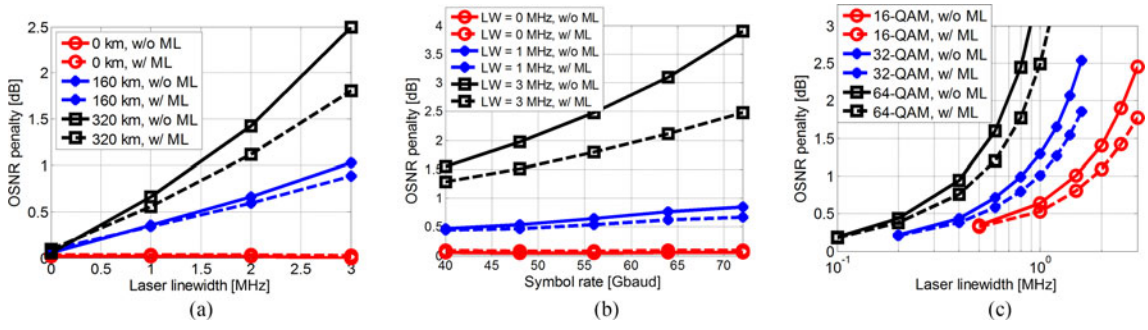

Meng Qiu et al., "Equalization-Enhanced Phase Noise in Stokes-Vector Direct-Detection Systems," Optical Fiber Communications Conference and Exhibition (OFC), 20-24 March 2016. © 2016 IEEE ISBN: 978-1-9435-8007-1
Reprinted with permission from IEEE

IEEE photonics SOCIETY

IEEE

Equalization-Enhanced Phase Noise in Stokes-Vector Direct Detection Systems

Meng Qiu,[1] Qunbi Zhuge,[1,2] Mohammed Y. S. Sowailem,[1] Thang M. Hoang,[1] Mathieu Chagnon,[1] Meng Xiang,[1,3] Xingyu Zhou,[1,4] Fangyuan Zhang,[1] and David V. Plant[1]

[1]Department of Electrical and Computer Engineering, McGill University, Montreal, QC H3A 0E9, Canada
[2]Ciena Corporation, Ottawa, ON K2H 8E9, Canada
[3]Wuhan National Laboratory for Optoelectronics, Huazhong University of Science and Technology, Wuhan 430074, China
[4]University of Electronic Science and Technology of China, Chengdu 611731, China

DOI:10.1109/JPHOT.2016.2628199

Manuscript received October 11, 2016; accepted November 8, 2016. Date of publication December 1, 2016; date of current version December 8, 2016. Corresponding author: Q. Zhuge (e-mail: qunbi.zhuge@mcgill.ca).

Abstract: In this work, we provide both numerical and experimental investigations of equalization-enhanced phase noise (EEPN) in Stokes-vector direct detection (SV-DD) systems. We show that the influence of EEPN cannot be neglected in high symbol rate SV-DD systems after transmission over several hundred kilometers of fibers when electronic chromatic dispersion compensation and lasers with linewidths of the order of Megahertz are employed. Simulation results are presented to evaluate the dependence of EEPN effects on laser linewidth, transmission distance, and symbol rate. Experiments are then conducted in a 56-Gbaud 16-quadrature amplitude modulation (QAM) SV-DD system to demonstrate the EEPN-induced performance degradation after 320-km transmission over standard single mode fiber (SSMF).

Index Terms: Phase modulation, optical fiber communication, Stokes parameters.

1. Introduction

Direct detection in Stokes space has been widely investigated in recent years because of its potential as a cost-effective solution for high-speed short-reach and medium-reach transmissions [1]–[6]. One specific configuration of Stokes space based detection is realized by sending modulated complex signals in one polarization and an accompanying carrier in the orthogonal polarization to achieve "self-coherent" detection at the receiver, which is denoted as Stokes-vector direct detection (SV-DD) system in this manuscript in accordance with the previous related works [3]–[6]. Such SV-DD systems can achieve the same spectral efficiency (SE) as single-polarization coherent transmission systems and avoid chromatic dispersion (CD) induced power fading [7], as well as signal-signal beat interference (SSBI) [8], [9] in the recovered signal. Based on the SV-DD system, 1-Tb/s transmission over 480-km standard single mode fiber (SSMF) has been demonstrated [5]. However, external cavity lasers (ECL) with small linewidths were employed in the previous demonstrations of SV-DD systems. Since one major motivation of the SV-DD scheme is the reduced cost, low-cost lasers are typically desired. Such lasers normally have relatively large laser linewidths of up to several MHz and their influence cannot be completely neglected in SV-DD systems.

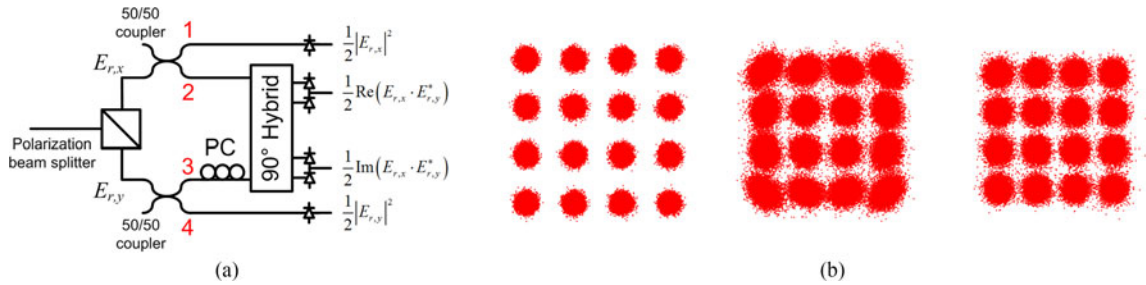

Fig. 1. (a) SVR structure. (b) Simulated constellations of the recovered 16-QAM symbols after 320-km transmission when the laser linewidth is 0 MHz (left), the laser linewidth is 3 MHz without ML phase compensation (middle), and the laser linewidth is 3 MHz with ML phase compensation (right). The OSNR is 32 dB and the symbol rate is 56 Gbaud.

In our previous work, we have numerically demonstrated that equalization-enhanced phase noise (EEPN) significantly degrades the signal quality after 320-km transmission in dispersion-unmanaged SV-DD systems when the transmitter laser has a linewidth of the order of MHz [10]. In this paper, we extend our studies in [10] and provide an experimental demonstration of the EEPN effects in a 56 Gbaud (224 Gb/s) 16-quadrature amplitude modulation (QAM) SV-DD system. In accordance with the simulation results, significant performance degradations are observed in the transmission experiments over 320-km SSMF when the transmitter ECL is replaced by distributed feedback (DFB) lasers with measured linewidths of 0.65 MHz and 1.6 MHz. In addition, more simulation results are provided to evaluate the dependence of the EEPN effects on laser linewidth, transmission distance, and symbol rate with various modulation formats. The remainder of this paper is organized as follows. In Section 2, the receiver structure of SV-DD systems is briefly described, followed by an explanation of the origin of EEPN in SV-DD systems. Then, in Section 3, the simulation and experiment setups are outlined. The results and discussions are then provided. Finally, we conclude in Section 4.

2. EEPN in SV-DD Systems

In the SV-DD system discussed in this work, we assume that the complex signal (S) is modulated in X polarization and a carrier (C) is transmitted in Y polarization. The corresponding Stokes vector can be represented as $\mathbf{S_t} = [S_{t,1}, S_{t,2}, S_{t,3}]^T = [|S|^2 - |C|^2, 2\mathrm{Re}(S \cdot C^*), 2\mathrm{Im}(S \cdot C^*)]^T$, where Re(·) and Im(·) represent the real and imaginary part of a complex number, respectively; the superscript T stands for transpose; and $*$ represents complex conjugate. Correspondingly, the polarization rotation during the propagation over fiber can be characterized in the Stokes space by a 3×3 matrix $\mathbf{R}$. At the receiver, the Stokes parameters of the received waveform are measured. One specific receiver structure to realize this measurement is illustrated in Fig. 1(a) [3]. Note that the second and third branch of this Stokes-vector receiver (SVR) achieves "self-coherent" detection analogous to a conventional coherent reception. Neglecting the scaling coefficients, the received Stokes vector $\mathbf{S_r}$ is obtained after the SVR, i.e., $\mathbf{S_r} = [S_{r,1}, S_{r,2}, S_{r,3}]^T = [|E_{r,x}|^2 - |E_{r,y}|^2, 2\mathrm{Re}(E_{r,x} \cdot E_{r,y}^*), 2\mathrm{Im}(E_{r,x} \cdot E_{r,y}^*)]^T$, where $E_{r,x(y)}$ represents the received waveform of $X(Y)$ polarization. After the matrix $\mathbf{R}$ is estimated, the transmitted Stokes vector can be recovered as $\hat{\mathbf{S}}_\mathbf{t} = \mathbf{R}^{-1} \times \mathbf{S_r} = [\hat{S}_{t,1}, \hat{S}_{t,2}, \hat{S}_{t,3}]^T$, where $\mathbf{R}^{-1}$ is the inverse matrix of $\mathbf{R}$. Finally, the modulated signal can be re-constructed based on $\hat{S}_{t,2}$ and $\hat{S}_{t,3}$. Since the signal and carrier experience same phase noise from the transmitter laser, the recovered waveform after the "self-coherent" detection has neither residual phase noise nor frequency offset in an ideal back-to-back scenario. Therefore, carrier recovery algorithms are normally not required in the digital signal processing (DSP) of SV-DD systems.

On the other hand, EEPN has been widely investigated in high data rate coherent long-haul transmission systems [11]–[14]. Specifically, assuming electronic CD post-compensation is employed, the local oscillator (LO) phase noise experienced by the received signal will interact with the CD equalizer. Such interplay disables perfect CD compensation and further induces extra amplitude

noise to the signal. A detailed analysis of EEPN has been provided in [11], which showed that the strength of EEPN scales with accumulated CD, symbol rate and laser linewidth. Similarly, the EEPN in SV-DD systems is related to the interplay between transmitter laser phase noise and a non-zero net dispersion assuming electronic CD post-compensation is employed. Specifically, the phase noise in the complex signal is dispersed with the waveform during transmission while the phase noise in the carrier is almost unaffected, so the signal and carrier exhibit different phase noise when they arrive at the receiver. As a result, residual phase perturbations are induced after the "self-coherent" detection, which can further be converted to amplitude noise after CD compensation. Note that although the target transmission distance of SV-DD systems is typically within hundreds of kilometers, which is much shorter than the long-haul schemes, a significant influence of EEPN is still possible if low-cost lasers with relatively large linewidths (e.g., several MHz) are employed.

Fig. 1(b) qualitatively illustrates the impact of EEPN in a simulated 56 Gbaud 16-QAM SV-DD system after 320-km transmission, and the details of the simulation parameters are presented in Section 3.1. Both enhanced amplitude noise and residual phase noise are observed in the presence of EEPN when the laser linewidth is 3 MHz. Specifically, the enhanced amplitude noise results in a spread of the symbol constellation, and the residual phase noise makes the constellation points non-circular.

In [10] we proposed to mitigate the EEPN induced performance degradation by employing maximum-likelihood (ML) phase estimation before symbol decoding as

$$H_k = \sum_{n=k-N}^{k+N} r_n (r_n)_D^* \tag{1}$$

$$\phi_k^{ML} = \tan^{-1}[\mathrm{Im}(H_k)/\mathrm{Re}(H_k)] \tag{2}$$

where r_n represents the n^{th} received symbol, N is the half width of the moving average filter, and $(\cdot)_D^*$ represents the complex conjugate of the symbol decision [15]. Then, the phase estimation ϕ_k^{ML} is applied to compensate the residual phase noise of the received symbols.

3. Results and Discussions

3.1 Simulations

Simulations are first conducted in MATLAB to investigate the dependence of EEPN strength on various system parameters. The symbol rate is 56 Gbaud and the modulation format is 16-QAM, unless specified otherwise. Root-raised cosine (RRC) pulse shaping with a roll-off factor of 0.1 is applied to the transmitted signal. The carrier-to-signal power ratio (CSPR) is 0 dB. The laser phase noise is modeled as a Wiener process [16] and added to the transmitted signal and carrier. SSMF with a dispersion parameter $D = 17$ ps/(nm·km) is assumed. The transmission impairments other than CD are not included in simulations. A noise-loading function is employed before the SVR to adjust the optical signal-to-noise ratio (OSNR) by changing the power of the loaded additive white Gaussian noise (AWGN). In this work, we consider the total power of the transmitted signal and the carrier as the "signal" power in the OSNR calculation. Since no polarization related impairments are included in simulations, the complex signal can be directly re-constructed based on $S_{r,2}$ and $S_{r,3}$. Then CD is compensated and matched filtering is applied. The ML phase compensation with $N = 12$ is also optionally employed, and this value of N enables near-optimum performance for various investigated cases. Finally, the BER is calculated after symbol decoding.

Fig. 2(a) depicts the OSNR penalty as a function of transmitter laser linewidth for different transmission distances. The OSNR penalty is obtained by calculating the difference between the simulated required OSNR at a BER of 3.8×10^{-3} in each case and that in the back-to-back scenario with a laser linewidth of 0 MHz. No OSNR penalty is observed in the back-to-back case with a laser linewidth of up to 3 MHz, indicating the high laser linewidth tolerance of SV-DD systems without the impact of EEPN. However, after transmission, EEPN starts affecting the performance when

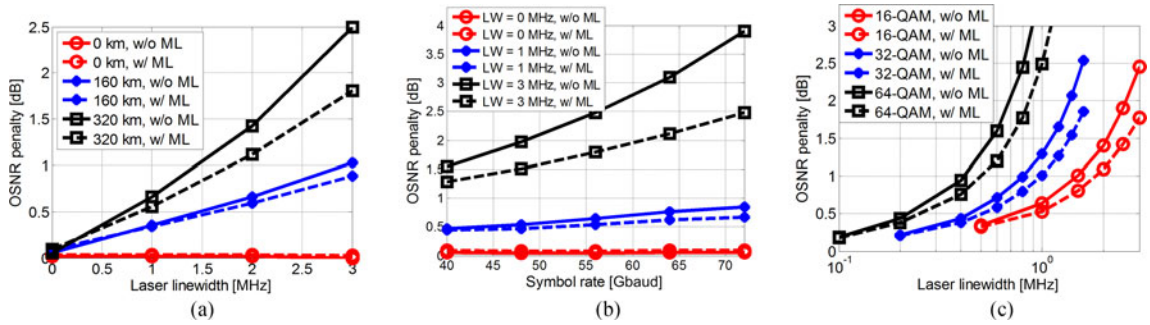

Fig. 2. (a) Simulated OSNR penalty versus laser linewidth in a 56 Gbaud 16-QAM system. (b) Simulated OSNR penalty versus symbol rate in a 16-QAM system after 320-km transmission. (c) Simulated OSNR penalty versus laser linewidth in 56 Gbaud systems with various modulation formats after 320-km transmission.

the laser linewidth is non-zero, and the performance degradation becomes more significant with increasing laser linewidths and transmission distances. Specifically, with a laser linewidth of 3 MHz, an OSNR penalty of 1 dB and 2.5 dB is observed when the transmission distance is 160 km and 320 km, respectively. When the ML phase compensation is employed, the OSNR penalty is reduced to 0.9 dB and 1.8 dB in these two cases, respectively. The performance improvement benefited from the ML phase compensation is also demonstrated by the recovered symbol constellation in Fig. 1(b), which shows that the residual phase errors can be effectively compensated.

Then we conduct more simulations by changing symbol rate and modulation format. Fig. 2(b) shows the OSNR penalty as a function of symbol rate with a transmission distance of 320 km. The EEPN induced OSNR penalty is more significant for higher symbol rates. Specifically, with a laser linewidth of 3 MHz, the OSNR penalty increases from 1.55 dB to 3.9 dB as the symbol rate increases from 40 Gbaud to 72 Gbaud. With the ML phase compensation, the OSNR penalty is reduced to 1.3 dB and 2.5 dB in these two cases, respectively. Finally, the laser linewidth tolerance after 320-km transmission is investigated for 16-QAM, 32-QAM, and 64-QAM formats, as shown in Fig. 2(c). As a result of EEPN, the laser linewidth tolerance at 1-dB OSNR penalty is limited to 1.5 MHz, 0.8 MHz and 0.4 MHz for 16-QAM, 32-QAM, and 64-QAM, respectively. Therefore, the influence of EEPN cannot be neglected in high symbol rate SV-DD systems where low-cost lasers with linewidths of the order of MHz are employed. When the ML phase compensation is employed, the laser linewidth tolerance increases to 1.8 MHz, 1 MHz, and 0.5 MHz for the three modulation formats, respectively.

3.2 Experiments

Fig. 3 outlines the setup for the experimental demonstration of the EEPN effects. The symbol rate is 56 Gbaud, and the modulation format is 16-QAM. Sixty four training symbols (TS) with non-return-to-zero (NRZ) pulse shape and a periodic pattern of $[0, 1, -1, 0, i, -i](i = \sqrt{-1})$ are inserted before the 16-QAM symbols for the purpose of estimating the polarization rotation matrix. The symbol rate for the training symbols is 437.5 Mbaud such that the accumulated CD after 320-km transmission imposes tolerable distortions on the training symbols. After the RRC pulse shaping for the 16-QAM signal and the re-sampling to the sampling rate of the digital-to-analog converters (DAC), the nonlinear response of the modulator and the frequency response due to the limited bandwidth of the transmitter components are pre-compensated. Finally, the samples are loaded to the DACs to generate signals for X polarization. Each DAC has a resolution of 8 bits and a sampling rate of 64 GSa/s. The signals are then modulated into optical domain by a dual polarization (DP) IQ modulator with a carrier wavelength of 1554.54 nm. Specifically, the outputs of the DACs are amplified and modulated to X polarization. For Y polarization, constant bias voltages which determine the transmittance of the modulator are applied, and the output power of the transmitted

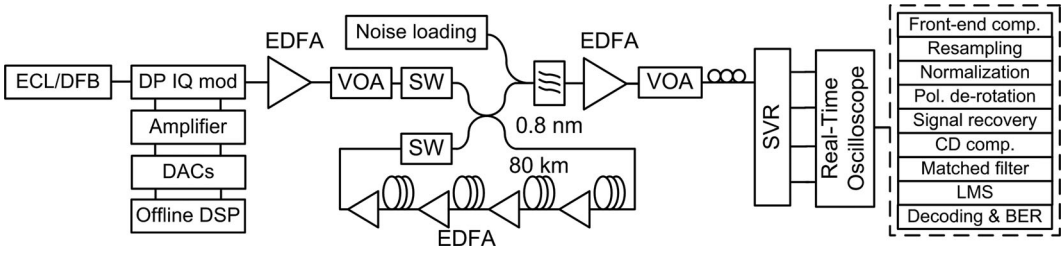

Fig. 3. Experiment setup. SW: switch.

carrier is adjusted to arrive at a CSPR of 0 dB. After the transmitter, the waveforms are amplified and pass through a variable optical attenuator (VOA) which controls the optical launch power. The propagation is realized in four spans of 80-km SSMF and EDFAs are employed to compensate the power losses. The total launch power of the modulated signal and the carrier is set as 3 dBm, which is optimized by minimizing the BER after transmission. Then the received waveforms are detected by a SVR. Inside the SVR, we use two 90/10 couplers in the experiments instead of the 50/50 couplers shown in Fig. 1(a). More power is assigned to the second and third branch because of the extra losses in these paths, e.g., the loss of the optical hybrid. Polarization controllers (PC) are used to align the polarizations of the second and third branch. A variable optical delay line (VODL) is also deployed in the third branch to synchronize the received waveforms with the 2nd branch. After the SVR, the waveforms are captured by a 4-channel real-time oscilloscope (RTO) with a sampling rate of 80 GSa/s per channel. The processing of the saved waveforms is performed offline in MATLAB. Specifically, the imbalance between channels is first compensated, followed by the re-sampling to 2 samples per symbol. The training symbols are then utilized to estimate the 3×3 channel rotation matrix in the Stokes space, and all of the received waveforms are de-rotated accordingly based on the inverse of the rotation matrix. Note that the channel response is stable for our processed samples, so de-rotating the signal once is already sufficient for effective processing. Afterwards, the complex modulated signal is recovered using $\hat{S}_{t,2}$ and $\hat{S}_{t,3}$. The following DSP functions include CD compensation, matched filtering, TS-aided least mean squares (LMS) equalizer, ML phase compensation, symbol decoding, and BER calculation.

To demonstrate the EEPN effects, we compare the system performances with three different transmitter lasers: a) an ECL with a measured linewidth of $<$20 kHz; b) a DFB laser with a measured linewidth of 0.65 MHz, denoted as DFB1; and c) a DFB laser with a measured linewidth of 1.6 MHz, denoted as DFB2. To measure the laser linewidth, we first connect these lasers in a coherent back-to-back system and use the measurement method proposed in [17]. Fig. 4(a) and 4(b) compare the BER versus OSNR measurements in the back-to-back case and after 320-km transmission. Simulation results are also plotted as reference (the solid lines and dashed lines correspond to the configuration without and with the ML phase compensation, respectively). In these simulations, extra AWGN is added to the signal to emulate the implementation penalty in the experiments, and the power of the AWGN is adjusted to line up the results between simulation and experiment when the ECL is employed. As shown in Fig. 4(a), the measured back-to-back performances are almost the same for different lasers, which is attributable to the removal of laser phase noise during the signal detection. This observation is in accordance with the simulation results in Fig. 4(a), where the simulated curves with different lasers completely overlap. However, after 320-km transmission, EEPN shows its impact, leading to a significant performance difference in experiments when different transmitter lasers are employed, as shown in Fig. 4(b). Meanwhile, the red, blue and black curves in Fig. 4(b) represent the simulation results when ECL, DFB1 and DFB2 are employed as the transmitter laser, respectively. Good matches between the simulation and experiment results are observed for DFB1, while a slight mismatch is observed for DFB2, which may be attributable to an underestimation of the laser linewidth in the experiment or the inaccuracy of emulating the implementation penalty using the aforementioned AWGN in this case. When the DFB lasers are employed, a very slight performance improvement is observed by employing the

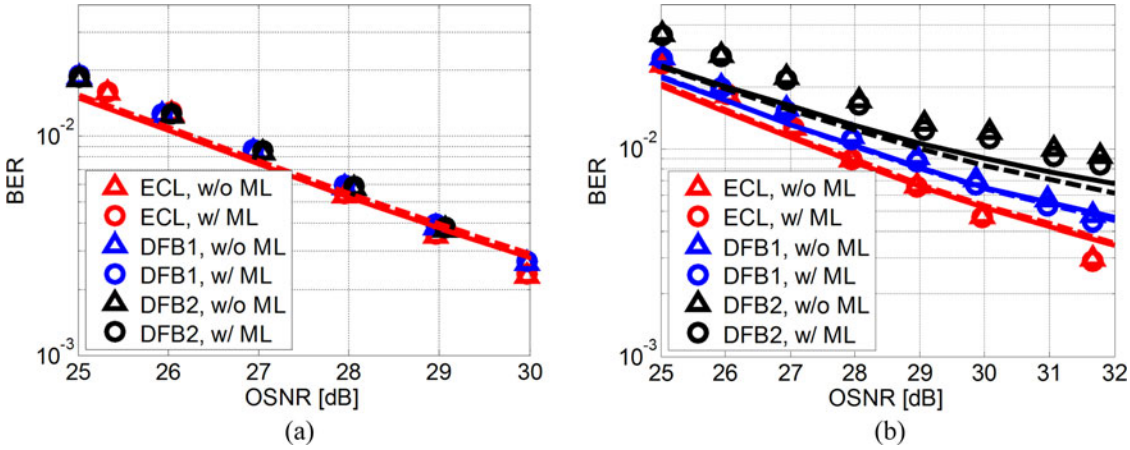

Fig. 4. Measured BER versus OSNR with different transmitter lasers (a) in back-to-back scenario and (b) after 320 km of transmission. The red, blue, and black solid (dashed) lines represent the simulation results without (with) ML phase compensation when ECL, DFB1, and DFB2 are employed as the transmitter laser, respectively.

ML phase compensation in both simulation and experiment results. The improvement is limited as the laser linewidth in our experiment is not very large. More significant performance improvement is expected when lasers with larger linewidth are adopted as demonstrated in the simulation results in Fig. 2.

4. Conclusion

In this work, we numerically and experimentally investigate the EEPN effects in SV-DD systems. We show that EEPN causes noticeable performance degradation in high symbol rate SV-DD systems after hundreds of kilometers transmission when a transmitter laser with a linewidth on the order of MHz is employed. In addition, we demonstrate that this EEPN-induced performance penalty can be partially mitigated by a simple ML phase compensation in the receiver-side DSP.

References

[1] K. Kikuchi, "Simple and efficient algorithm for polarization tracking and demultiplexing in dual-polarization IM/DD systems," in *Proc. OFC*, 2015, paper Th1E.3.
[2] M. Morsy-Osman, M. Chagnon, M. Poulin, S. Lessard, and D. V. Plant, "224-Gb/s 10-km transmission of PDM PAM-4 at 1.3 μm using a single intensity-modulated laser and a direct-detection MIMO DSP-based receiver," *J. Lightw. Technol.*, vol. 33, no. 7, pp. 1417–1424, Apr. 2015.
[3] D. Che, A. Li, X. Chen, Q. Hu, Y. Wang, and W. Shieh, "Stokes vector direct detection for short-reach optical communication," *Opt. Lett.*, vol. 39, no. 11, pp. 3110–3113, Jun. 2014.
[4] W. Shieh, D. Che, Q. Hu, and A. Li, "Linearization of optical channels with Stokes vector direct detection," in *Proc. OFC*, 2015, paper Th1E.5.
[5] D. Che, Q. Hu, X. Chen, A. Li, and W. Shieh, "1-Tb/s Stokes vector direct detection over 480-km SSMF transmission," in *Proc. OECC*, 2014, paper THPDP1-2.
[6] D. Che, A. Li, Q. Hu, X. Chen, and W. Shieh, "Implementing simplified stokes vector receiver for phase diverse direct detection," in *Proc. OFC*, 2015, paper Th1E.4.
[7] Y. Gao, Q. Zhuge, W. Wang, X. Xu, J. M. Buset, M. Qiu, M. Morsy-Osman, M. Chagnon, F. Li, L. Wang, C. Lu, A. P. T. Lau, and D. V. Plant, "40 Gb/s CAP32 short reach transmission over 80 km single mode fiber," *Opt. Exp.*, vol. 23, no. 9, pp. 11412–11423, Apr. 2015.
[8] D. Che, Q. Hu, and W. Shieh, "Linearization of direct detection optical channels using self-coherent subsystems," *J. Lightw. Technol.*, vol. 34, no. 2, pp. 516–524, Jan. 2016.
[9] Y. Wang, J. Yu, and N. Chi, "Demonstration of 4 $\times$ 128-Gb/s DFT-S OFDM signal transmission over 320-km SMF with IM/DD," *IEEE Photon. J.*, vol. 8, no. 2, pp. 1–9, Apr. 2016.
[10] M. Qiu, Q. Zhuge, M. Chagnon, and D. V. Plant, "Equalization-enhanced phase noise in Stokes-vector direct detection systems," in *Proc. OFC*, 2016, paper Th2A.35.

[11] W. Shieh and K.-P. Ho, "Equalization-enhanced phase noise for coherent-detection systems using electronic digital signal processing," *Opt. Exp.*, vol. 16, no. 20, pp. 15718–15727, Sep. 2008.
[12] A. P. T. Lau, T. S. R. Shen, W. Shieh, and K.-P. Ho, "Equalization-enhanced phase noise for 100 Gb/s transmission and beyond with coherent detection," *Opt. Exp.*, vol. 18, no. 16, pp. 17239–17251, Jul. 2010.
[13] G. Jacobsen, T. Xu, S. Popov, J. Li, A. T. Friberg, and Y. Zhang, "EEPN and CD study for coherent optical nPSK and nQAM systems with RF pilot based phase noise compensation," *Opt. Exp.*, vol. 20, no. 8, pp. 8862–8870, Apr. 2012.
[14] Q. Zhuge *et al.*, "Experimental investigation of the equalization-enhanced phase noise in long haul 56 Gbaud DP-QPSK systems," *Opt. Exp.*, vol. 20, no. 13, pp. 13841–13846, Jun. 2012.
[15] X. Zhou, "An improved feed-forward carrier recovery algorithm for coherent receivers with M-QAM modulation format," *IEEE Photon. Technol. Lett.*, vol. 22, no. 14, pp. 1051–1053, Jul. 2010.
[16] M. G. Taylor, "Phase estimation methods for optical coherent detection using digital signal processing," *J. Lightw. Technol.*, vol. 27, no. 7, pp. 901–914, Apr. 2009.
[17] X. Chen, A. A. Amin, and W. Shieh, "Characterization and monitoring of laser linewidths in coherent systems," *J. Lightw. Technol.*, vol. 29, no. 17, pp. 2533–2537, Sep. 2011.